GEM-QUALITY SERPENTINE FROM VAL MALENCO, CENTRAL ALPS, ITALY

Ilaria Adamo, Valeria Diella, Rosangela Bocchio, Caterina Rinaudo, and Nicoletta Marinoni

Pizzo Tremogge in Val Malenco, Italy, is a source of gem-quality serpentine. Samples from this mountain locality were investigated by standard gemological and petrological methods, Raman spectroscopy, and electron microprobe analysis. The rough and polished specimens were massive aggregates, with a green to yellow color and white, gray, and black veins or spots. From a mineralogical standpoint, this material consists of all three phases of serpentine-group minerals (lizardite, antigorite, and chrysotile) alternating with other minerals such as carbonate (calcite and dolomite), quartz, chlorite, and brucite. The quantity of carved and polished material to date is small, but the latest geological prospecting indicates the outcrop's strong potential.

Serpentine-group minerals are common rock-forming hydrous phyllosilicates, with an ideal chemical formula of $Mg_3Si_2O_5(OH)_4$. Each of the three main serpentine polymorphs (chrysotile, lizardite, and antigorite) forms under a wide range of thermic conditions in many geologic settings (Evans et al., 2013). *Serpentinite*[1], which consists mostly of serpentine-group minerals, has been used since antiquity for ceremonial and ornamental carvings (Guillot and Hattori, 2013). Gem-quality serpentine, often referred to as "noble" serpentine, is characterized by a compact microstructure and fine colors, such as blue-green, yellowish green, gray, and white (O'Donoghue, 2006). The material is sometimes used as an imitation of jadeite and nephrite because of its similar aggregate structure and color appearance, and it is often marketed as "serpentine jade" (Kim et al., 2006; Lin et al., 2012). A rare chatoyant variety of serpentine was also reported by Choudhary (2009).

Val Malenco (or Malenco Valley) in the Central Alps of Italy, famous for gem-quality demantoid, nephrite, and rhodonite (Adamo et al., 2009; Adamo and Bocchio, 2013; Diella et al., 2014), is also a source of gem-quality serpentine (figure 1). In particular, one of Val Malenco's best-known sources for serpentine is Pizzo Tremogge (or Tremogge Peak) (figure 2, left). As seen in figure 2, right, serpentine is included in forsterite olivine-bearing marbles from the Paleozoic era (Bedogné et al., 1993).

Gem-quality serpentine from Pizzo Tremogge was discovered by mineral collector Pietro Sigismund, who reported the find in the 1930s (Gramaccioli, 1962). Production and marketing of the material started around the year 2000 (P. Nana, pers. comm., 2015). The serpentine layers (figure 3), located 2800 m above sea level, are discontinuous (up to 300–350 m in length and 40 m in thickness), and mining is limited by difficult access. Although the outlook for future production is uncertain, reserves at deeper layers may be inferred.

Serpentine from Pizzo Tremogge was traditionally identified as lizardite, although a full mineralogical investigation of this material has yet to be conducted. Recent preliminary data by Adamo et al. (2014) proved that antigorite and chrysotile also occur together with lizardite. Therefore, it seems useful to provide a further detailed characterization of the serpentine from

See end of article for About the Authors and Acknowledgments.
GEMS & GEMOLOGY, Vol. 52, No. 1, pp. 38–49,
http://dx.doi.org/10.5741/GEMS.52.1.38

[1] *Serpentinite*: Rock consisting largely of serpentine-group minerals formed by "serpentinization," a process consisting of a hydration and metamorphic transformation of oceanic crustal and upper mantle material.

Figure 1. Serpentine from Pizzo Tremogge in Val Malenco, Italy. Left: A bead necklace rests on a 15 cm long ornamental polished slab. The necklace is accompanied by a cat statuette measuring about 4 cm high and two pendants approximately 3.5–4 cm in length. The necklace on the right consists of spherical beads ranging in diameter from 1.0 to 2.0 cm. Photos by Pietro Nana.

Pizzo Tremogge, focusing on its use as a gem material. We investigated a suite of rough and cut samples provided by Mr. Pietro Nana (Sondrio, Italy), using gemological characterization, electron microprobe chemical analyses, and Raman spectroscopy. The latter is a reliable and nondestructive method for identifying the three serpentine minerals (Rinaudo et al., 2003).

BACKGROUND INFORMATION

Serpentine-group minerals include lizardite, chrysotile, and antigorite, which are polymorphs of the Mg-rich hydrous phyllosilicate with the approximate chemical formula $Mg_3Si_2O_5(OH)_4$. To some extent, Fe, Al, and Ni may be substituted for antigorite, and Al for Si (Deer et al., 2009). The basic structural unit

Figure 2. Left: A view of Pizzo Tremogge in Val Malenco, Italy. Photo by Pietro Nana. Right: A sketch map of the Pizzo Tremogge area, showing (1) clinothulite outcrop (in dark brown), (2) "noble" serpentine layers (in light brown), (3) marbles with olivine (forsterite), and (4) marbles with intercalations of "noble" serpentine. Modified from Gramaccioli (1962).

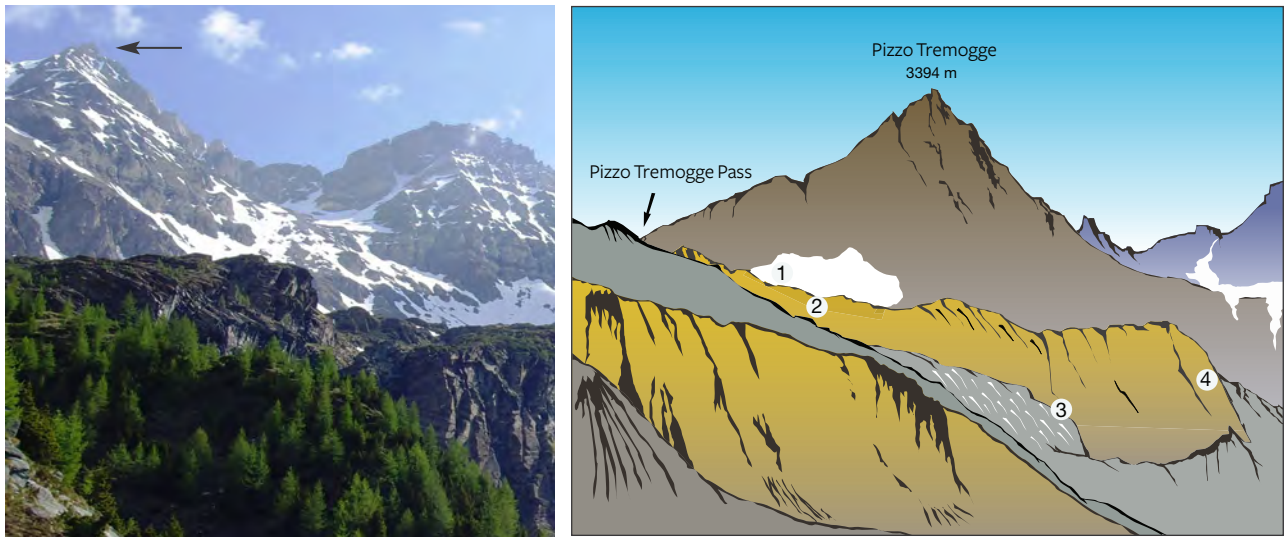

Figure 3. The serpentine layers intercalated with marble at Pizzo Tremogge. Photo by Pietro Nana.

consists of an Mg-rich sheet, linked on one side to a single tetrahedral silicate sheet, with hydrogen bonding between the layers (Evans et al., 2013). Lizardite, chrysotile, and antigorite are distinguished by their crystal microstructure, consisting of different arrangements of the layers. Lizardite and chrysotile are characterized by a flat and a curved/cylindrical crystal microstructure, respectively, while antigorite displays wavy layers resulting in a corrugated microstructure (Evans et al., 2013). Serpentine minerals form by the hydration of olivine-rich ultramafic rocks at relatively low temperature; this is the serpentinization process. The three serpentine-group minerals have different stability fields (Deer et al., 2009). In particular, lizardite is the first phase that commonly pseudomorphs after olivine; chrysotile occurs mainly as a filling in the fractures that crosscut serpentinite rocks, whereas antigorite is considered the high-temperature phase, growing from lizardite and chrysotile with increasing grade of metamorphism at temperatures above about 320°C (Evans et al., 2013). Chrysotile is also the main constituent of commercial asbestos, which was used extensively for thermal and electric insulation until the discovery that its fine dust is harmful to human health (Fubini and Fenoglio, 2007).

In Brief

- Gem serpentine is a massive aggregate of hydrous magnesium silicate crystals.
- Serpentine from Pizzo Tremogge, in Val Malenco of the Italian Central Alps, has been known since the 1930s but was not marketed until about 2000.
- Samples from this locality consist of all three phases of serpentine-group minerals, alternating with other mineral phases.

GEOLOGICAL SETTING

Val Malenco is located at the border of southeastern Switzerland and northern Italy, between the Penninic and the Austroalpine domains of the Alps (Müntener et al., 2000). The regional geology appears complex due to extensive tectonic disruption associated with a stack of Alpine nappes (Penninic and Austroalpine nappe system). Three major structural complexes, shown in figure 4 from east to west, characterize this area:

1. the Margna unit, composed of basement rocks with a Mesozoic sedimentary cover
2. the Malenco unit, one of the largest *ultramafic*[2] masses of the Alps, dominated by variably serpentinized ultramafic rocks

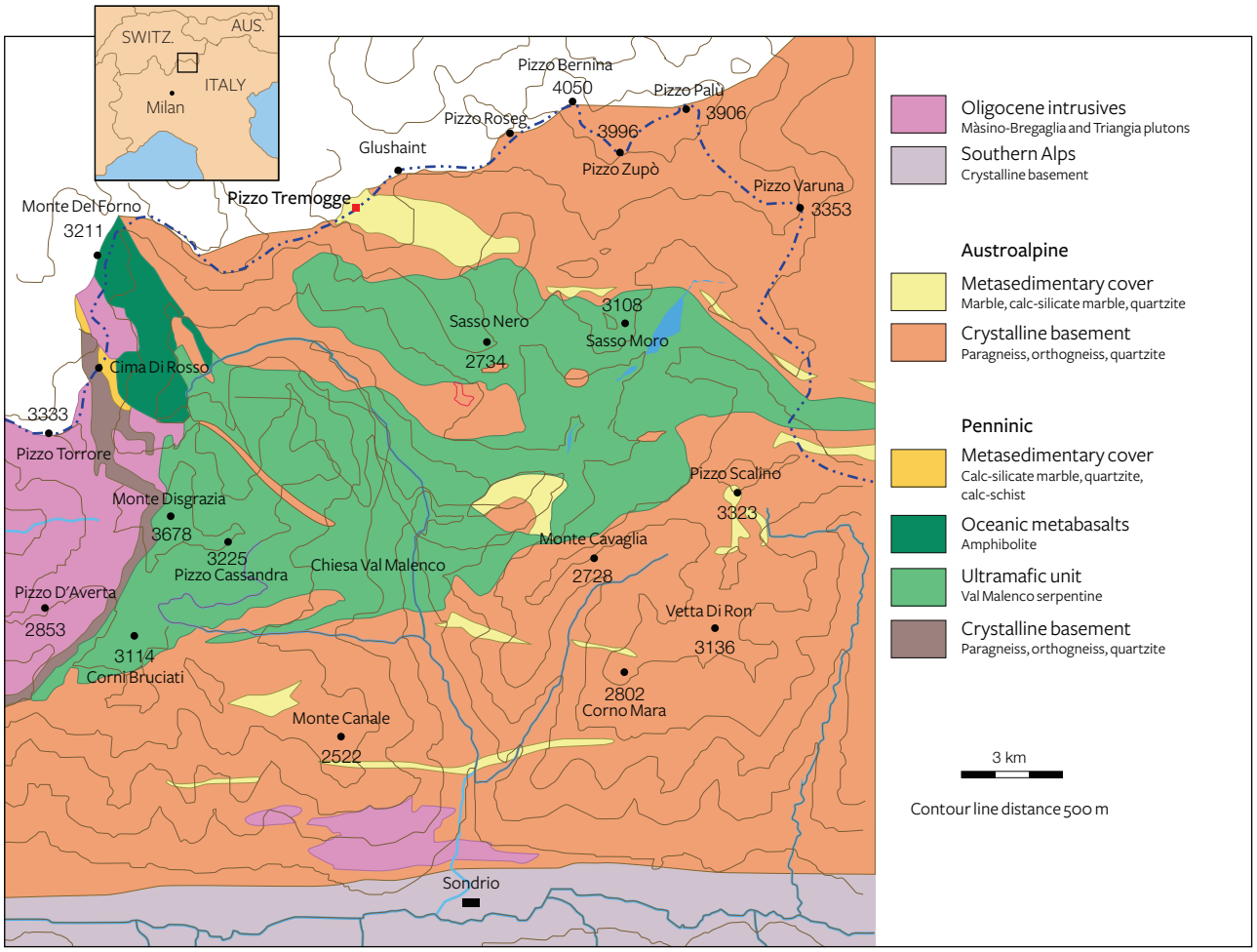

Figure 4. This geological map of Val Malenco shows the rocks constituting the Margna unit (brown and light yellow), the Malenco unit (dark green), and the Monte del Forno unit (light green). Gem-quality serpentine is found in the metasedimentary cover, consisting mainly of marbles, of the Margna unit. Modified from Adamo et al. (2009).

3. the Monte del Forno unit, an *ophiolite*[3] suite, consisting of oceanic metabasaltic rocks

In the Margna unit, the crystalline basement rocks show intercalations of carbonate rocks both of Paleozoic and Mesozoic age (Bedogné et al., 1993). The more ancient lithologies consist mainly of calcite-bearing marbles that preserve the amphibolite-facies paragenesis conditions of the enclosing rocks (gneisses and metagabbros). The composition of these marbles is not homogenous and is mainly related to the different proportions of carbonate and other associated minerals. Marbles in the area of Pizzo Tremogge (again, see figure 2), located 2800 m above sea level, are multicolored (yellow, yellow-green, and brown-orange) and show a rich mineral content, with magnesium silicates (clinohumite, olivine, serpentine, diopside, chlorite, and phlogopite), spinel, graphite, hematite, pyrite, and brucite. In most cases, olivine (forsterite) is completely replaced by yellow-green serpentine and chlorite (Bedogné et al., 1993).

MATERIALS AND METHODS

A total of 10 samples from Pizzo Tremogge, consisting of four rough and six cut specimens (four spheres and two freeforms), were investigated in this study (see table 1 and figure 5).

Optical properties and specific gravities (SG) of

[2]*Ultramafic*: Igneous rock with low silica content (less than 45% SiO_2). Ultramafic rocks are usually composed of greater than 90% mafic minerals, which are typically dark and have high magnesium and iron contents.

[3]*Ophiolite*: From the Greek "ophio" (snake) and "lithos" (stone). Ophiolite sequences are brilliant green, snake-like stratified serpentine minerals that form in altered oceanic crust and mantle. While ophiolites are rare, occurrences are found in localities around the world.

the six cut samples were determined at the Italian Gemological Institute (IGI) laboratory in Milan using standard gemological methods. Refractive indices (RI) were measured by the distant vision method using a Kruss refractometer with sodium light (589 nm) from a Leitz lamp, and methylene iodide saturated with sulfur and C_2I_4 as a contact liquid (RI = 1.80). A Mettler hydrostatic balance was used to determine the SG. Ultraviolet fluorescence was investigated with a short-wave (254 nm) and long-wave (366 nm) UV lamp.

Raman spectroscopic analyses were carried out on four thin petrographic sections cut from samples S1, S2, S3, and S4) at the University of Eastern Piedmont in Alessandria, Italy, using a Jobin Yvon LabRam HR800 μ-Raman spectrometer equipped with an Olympus BX41 microscope, an HeNe 20 mW laser working at 632.8 nm, and a charge-coupled device (CCD) air-cooled detector. The instrument was calibrated by checking the position and intensity of the Si band at 520.65 ± 0.05 cm^{-1} before every run. In order to balance signal against noise, at least 50 cycles of 20 seconds each were performed. The spectral region recorded ranged from 1200 to 200 cm^{-1}, where the vibrational lattice modes of the different minerals are located. Spectra were acquired using Origin 6.0 data analysis software. The mineral phases responsible for the different Raman bands observed were identified by previously published Raman spectra (Kloprogge et al., 1999; Rinaudo et al., 2003; Groppo et al., 2006) and the RRUFF database (http://rruff.info).

Figure 5. These cut serpentines (7.35–13.78 ct) were among the samples investigated in this study. Photo by Rosangela Bocchio.

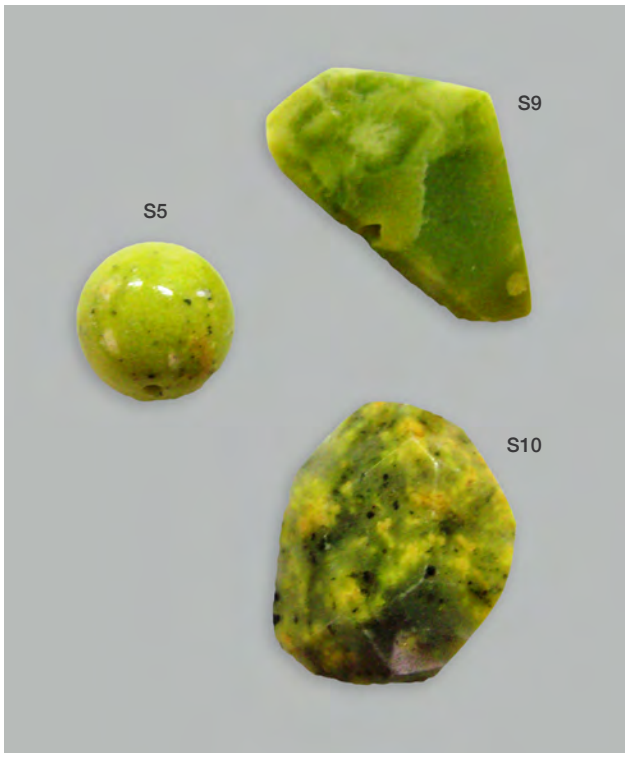

TABLE 1. Serpentine samples investigated in this study.

Sample	Appearance	Dimensions
S1	Thin section	4 × 2 cm
S2	Thin section	4 × 2 cm
S3	Thin section	4 × 2 cm
S4	Thin section	4 × 2 cm
S5	Sphere	1.02–1.05 cm diameter
S6	Sphere	1.06–1.07 cm diameter
S7	Sphere	1.04–1.05 cm diameter
S8	Sphere	1.02–1.03 cm diameter
S9	Freeform	1.30 × 2.23 × 0.60 cm
S10	Freeform	1.50 × 1.85 × 0.70 cm

Backscattered electron images and quantitative chemical analyses of major and minor elements were performed at the University of Milan on four polished thin sections (4 × 2 cm in dimension, cut from the rough samples S1, S2, S3, and S4) after a petrographic study by optical microscope. Quantitative chemical analysis was performed using a JEOL JXA-8200 electron microprobe in wavelength-dispersive mode, under operating conditions of 15 kV accelerating voltage, 5 nA beam current, and count times of 30 seconds on peaks and 10 seconds on the background. The following elements were measured: Na, Mg, Al, Si, K, Ca, Ti, V, Cr, Mn, Ni, Zn, and Fe. Natural minerals or pure metals were used as the standards, and the raw data were corrected for matrix effects using a conventional φρZ routine in the JEOL software package. Detection limits were 0.01 wt.%.

RESULTS AND DISCUSSION

Gemological Properties. The gemological properties of the six cut samples are reported in table 2. Serpentine from Pizzo Tremogge has a massive aspect, with a green to yellowish green to yellow color, sometimes with white or gray veins and black spots. The samples' spot RI was approximately 1.55, and SG ranged from 2.50 to 2.67, with variations related to the occurrence

of other minerals. In particular, specimens with many black inclusions had a higher SG. The data were consistent with those previously measured by Adamo et al. (2014) and within the range reported by O'Donoghue (2006). Moreover, the values of RI and SG matched those reported by Kim et al. (2006) for gem-quality serpentine jade from Korea, composed of antigorite (1.56 and 2.57, respectively). The SG of our specimens also corresponded with the values (2.50–2.73) measured by Lin et al. (2012) for serpentine jade from Jilin province in China, consisting of lizardite.

The serpentine samples from Pizzo Tremogge are inert to UV radiation and have a Mohs hardness of approximately 4, which is typical of serpentine (Kim et al., 2006; Xinying et al., 2012).

Petrographic Examination and Raman Spectroscopy. When observed with a petrographic microscope, the samples showed a coarse-grained structure. Serpentine was the dominant mineral, alternating with carbonate (calcite and dolomite), quartz, brucite, and chlorite veins (figure 6).

The identification of serpentine minerals (lizardite, antigorite, and chrysotile) through petrographic examination is difficult, owing to their similar optical properties as well as their submicroscopic intergrowths (Rinaudo et al., 2003; Groppo et al., 2006). Four samples (S1, S2, S3, and S4) were therefore examined by petrographic Raman spectroscopy to determine their mineralogical composition. The Raman spectra of the four serpentine thin sections are shown in figure 7, whereas table 3 presents the bands observed and their assignments.

Comparison of the Raman spectra of serpentine from Val Malenco (figure 7) with those reported in the literature for lizardite, chrysotile, and antigorite suggests the following:

- The spectrum of sample S1 shows an association of chlorite and lizardite. Since the thin petrographic sections are glued on the glass slide, resin is responsible for the bands at 1184, 1112, 1048, 821, 769, 736, and 639 cm^{-1} in the Raman spectrum. Repeated check analyses on the resin showed unequivocally the assignment of

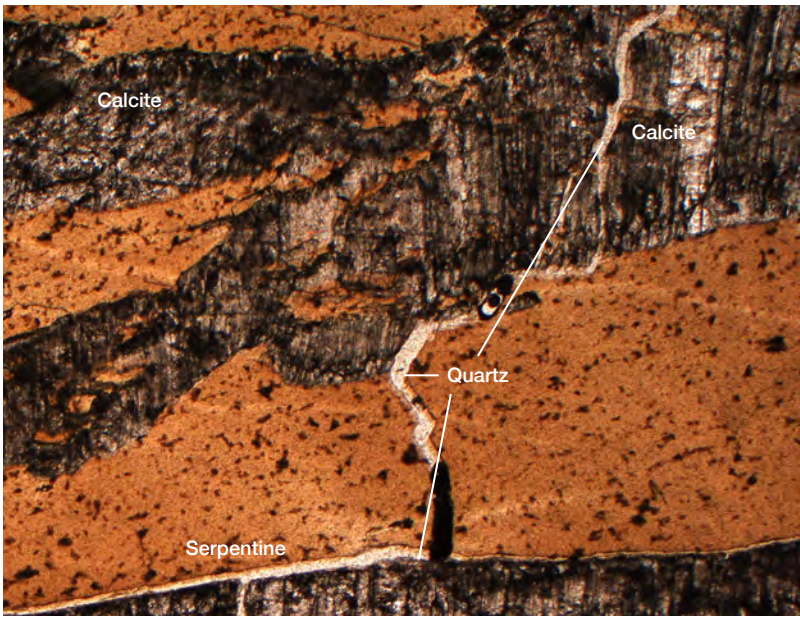

Figure 6. Observed in plane polarized light, this thin section of sample S2 shows serpentine (light brown), calcite (brown), and quartz veins (white). Photomicrograph by Rosangela Bocchio.

TABLE 2. Gemological properties of the fashioned serpentine samples.

Samples	S5	S6	S7	S8	S9	S10
Cut	Sphere	Sphere	Sphere	Sphere	Freeform	Freeform
Weight (ct)	7.35	8.01	7.50	7.47	9.81	13.78
Color	Greenish yellow	Greenish yellow	Greenish yellow	Yellow	Yellowish green	Greenish yellow
Diaphaneity	Opaque	Opaque	Opaque	Opaque	Opaque	Opaque
RI	1.55	1.55	1.55	1.55	1.55	1.55
SG	2.61	2.62	2.61	2.63	2.50	2.67
Mohs hardness	4	4	4	4	4	4
UV fluorescence	Inert	Inert	Inert	Inert	Inert	Inert

TABLE 3. Band frequency (cm^{-1}) and assignment in four serpentine samples.

Sample 1	Sample 2	Sample 3	Sample 4	Band assignment	Reference
—	1097	—	—	Lizardite	Rinaudo et al. (2003)
—	—	1105	1103	Chrysotile	Kloprogge et al. (1999)
—	—	1088	—	Calcite	White (2009)
—	—	1044	1044	Antigorite	Kloprogge et al. (1999), Petriglieri et al. (2015)
—	—	714	—	Calcite	White (2009)
—	691	693	692	Lizardite, chrysotile	Rinaudo et al. (2003) Petriglieri et al. (2015)
	—	688	—	Mixed antigorite-chrysotile	Groppo et al. (2006)
690	—	—	—	Chlorite-lizardite	Groppo et al. (2006), Prieto et al. (1991)
—	628	629	629	Lizardite, chrysotile	Rinaudo et al. (2003)
546	—	552	—	Chlorite	Prieto et al. (1991)
—	—	—	520	Antigorite	Rinaudo et al. (2003)
	—	463–464	464	Chrysotile, antigorite	Kloprogge et al. (1999), Groppo et al. (2006)
463	—	—	—	Chlorite	Prieto et al. (1991)
—	—	432	434	Chrysotile	Kloprogge et al. (1999)
388	392	391	390	Lizardite, chrysotile	Rinaudo et al. (2003), Petriglieri et al. (2015)
—	—	380	382	Antigorite	Groppo et al. (2006)
357	—	358	—	Chlorite	Prieto et al. (1991)
349	349	346	347	Lizardite, chrysotile	Rinaudo et al. (2003), Petriglieri et al. (2015)
—	—	321	321	Chrysotile	Kloprogge et al. (1999)
—	—	284	—	Calcite	White (2009)
284				Chlorite	Prieto et al. (1991)
238	235	230–234	232	Lizardite, chrysotile, antigorite	Rinaudo et al. (2003), Petriglieri et al. (2015)

"—": Peak is not present.

these peaks. The more intense band at 690 cm^{-1} is generated by the combination of the more intense bands of chlorite at 682–683 cm^{-1} (Prieto et al., 1991) and lizardite at 690–693 cm^{-1} (Rinaudo et al., 2003; Groppo et al., 2006). The presence of chlorite is confirmed by the observation of bands at 546, 463, 357, and 284 cm^{-1}; lizardite crystallization is indicated by the bands at 388 and 238 cm^{-1}. As demonstrated by Groppo et al. (2006), in lizardite the band near 390 cm^{-1} shifts toward lower wavenumbers, with increasing amounts of Al replacing Si in the tetrahedral sites. In our case, chemical microprobe analyses show a lower SiO_2 content in sample S1 (see the "Chemical Analysis" section and table 4).

- The spectrum of sample S2 is unequivocally assigned to lizardite. The band at 1097 cm^{-1} is unique to this variety of serpentine, whereas the bands at 691, 628, 392, 349, and 235 cm^{-1} are in the proximity of lizardite and chrysotile (Rinaudo et al., 2003; Petriglieri et al., 2015).
- Sample S3 was analyzed in two different areas due to an evident color variation in different

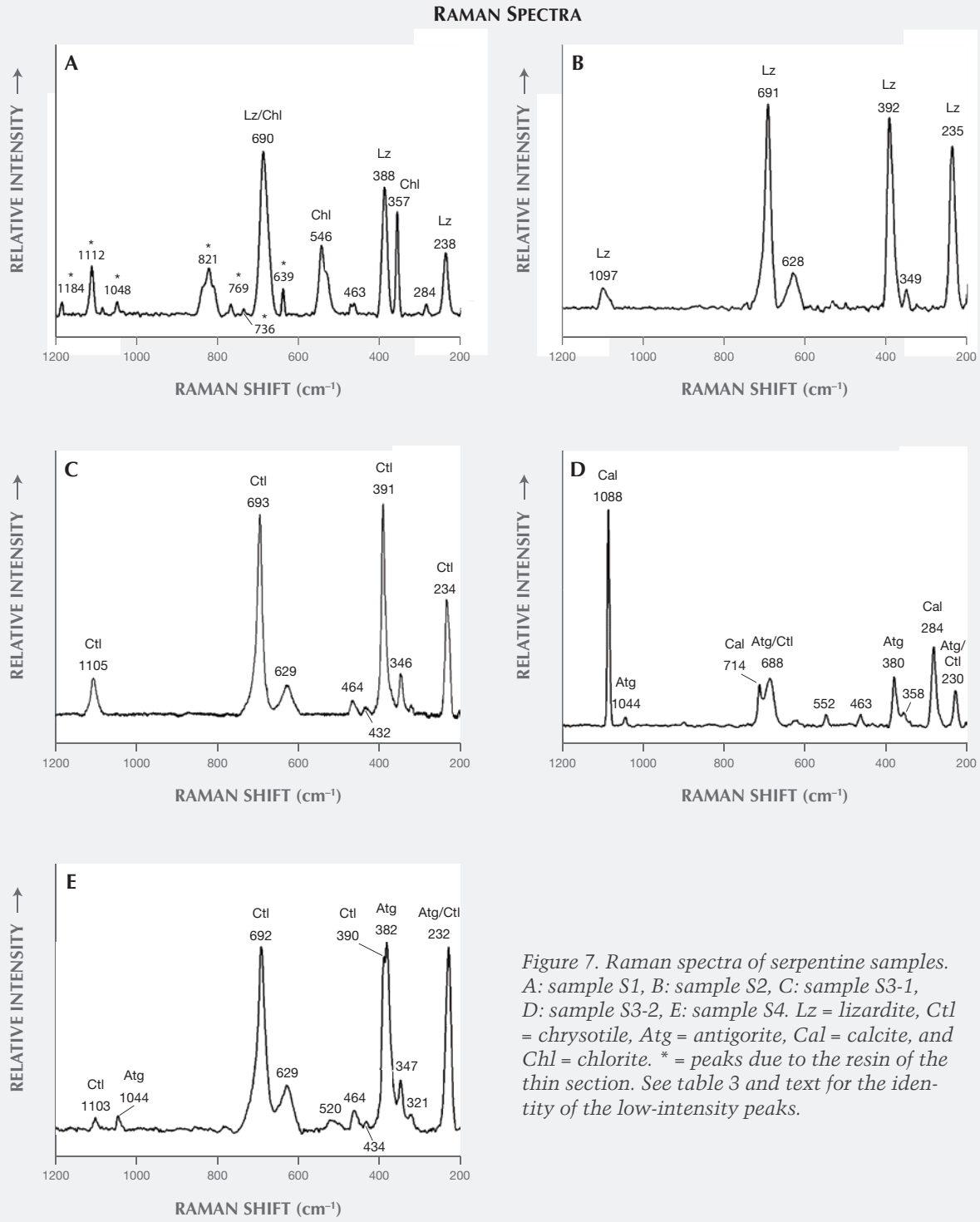

*Figure 7. Raman spectra of serpentine samples. A: sample S1, B: sample S2, C: sample S3-1, D: sample S3-2, E: sample S4. Lz = lizardite, Ctl = chrysotile, Atg = antigorite, Cal = calcite, and Chl = chlorite. * = peaks due to the resin of the thin section. See table 3 and text for the identity of the low-intensity peaks.*

areas of the stone. In the spectrum obtained from the greenish yellow area (figure 7C), the shape and the position of the single bands occurring at 1105, 693, 629, 391, 346, and 234 cm^{-1} correspond with those of pure chrysotile reported by Rinaudo et al. (2003) and Petriglieri et

TABLE 4. Microprobe analyses of four serpentine samples.

Sample wt.%	S1	S1	S2	S2	S2	S3	S3	S3	S4	S4	S4
SiO_2	40.55	40.37	39.81	40.21	40.31	42.66	42.86	42.73	41.52	43.26	43.20
TiO_2	0.12	0.17	0.21	0.14	0.16	0.12	0.15	0.15	0.11	0.14	0.07
Al_2O_3	2.16	2.23	3.13	3.08	3.13	1.19	1.21	1.23	1.01	0.66	0.72
Cr_2O_3	0.03	0.02	bdl	bdl	bdl	bdl	bdl	bdl	0.05	0.04	bdl
FeO	3.72	3.58	3.22	3.34	3.30	1.83	1.46	1.52	1.86	1.52	1.40
NiO	bdl	0.01	0.04	0.04	0.01	0.04	0.06	bdl	bdl	0.01	bdl
MnO	0.01	bdl	0.01	bdl	bdl	0.05	bdl	bdl	0.02	0.06	bdl
MgO	39.61	39.29	40.17	39.93	39.93	41.90	41.78	42.08	41.49	40.55	40.72
CaO	0.18	0.02	0.03	0.01	0.02	0.04	0.03	0.04	0.02	0.02	bdl
ZnO	bdl	bdl	0.02	bdl	0.08	0.05	0.04	bdl	0.08	0.09	0.09
Na_2O	bdl	bdl	0.01	0.01	bdl	bdl	bdl	0.02	0.01	bdl	bdl
K_2O	bdl	bdl	0.01	bdl	0.01	bdl	bdl	bdl	0.01	0.01	bdl
H_2O	12.62	12.54	12.69	12.72	12.74	13.00	13.00	13.01	12.73	12.84	12.83
Total	99.00	98.23	99.35	99.48	99.69	100.88	100.59	100.78	98.91	99.20	99.03
Tetrahedral cations											
Si^{4+}	1.925	1.929	1.881	1.897	1.897	1.969	1.978	1.969	1.957	2.022	2.020
Al^{3+}	0.075	0.071	0.119	0.103	0.103	0.031	0.022	0.031	0.043	–	–
Total	2.00	2.00	2.00	2.00	2.00	2.00	2.00	2.00	2.00	2.02	2.02
Octahedral cations											
Ti^{4+}	0.004	0.006	0.007	0.005	0.006	0.004	0.005	0.005	0.004	0.005	0.003
Al^{3+}	0.046	0.054	0.056	0.068	0.071	0.033	0.044	0.036	0.013	0.036	0.039
Cr^{3+}	0.001	0.001	–	–	–	–	–	–	0.002	0.001	–
Fe^{2+}	0.148	0.143	0.127	0.132	0.130	0.071	0.056	0.059	0.073	0.059	0.055
Ni^{2+}	–	–	0.002	0.001	0.001	0.001	0.002	–	–	0.001	–
Mn^{2+}	–	–	–	–	–	0.002	–	–	0.001	0.002	–
Mg^{2+}	2.803	2.798	2.830	2.808	2.802	2.882	2.875	2.891	2.915	2.825	2.839
Ca^{+}	0.009	0.001	0.002	0.001	0.001	0.002	0.001	0.002	0.001	0.001	–
Zn^{2+}	–	–	0.001	–	0.003	0.002	0.001	–	0.003	0.003	0.003
Na^{+}	–	–	0.001	0.001	–	–	–	0.002	0.001	–	–
K^{+}	–	–	0.001	–	–	–	–	–	–	0.001	–
Total	3.01	3.00	3.03	3.02	3.01	3.00	2.99	3.00	3.01	2.93	2.94
OH	4.00	4.00	4.00	4.00	4.00	4.00	4.00	4.00	4.00	4.00	4.00

bdl = below detection limit
"—": Peak is not present.

al. (2015). The bands detected at 464, 432, and 321 cm^{-1} can be assigned to chrysotile, in agreement with the spectrum obtained by Kloprogge et al. (1999). The spectrum recorded in the green area (figure 7D) shows a band at 1044 cm^{-1} that is ascribed unequivocally to antigorite because

it occurs in a frequency range where no band of chrysotile or lizardite is present (Rinaudo et al., 2003; Petriglieri et al., 2015). On the basis of the data from Groppo et al. (2006), bands at 463 and 380 cm^{-1} can also be assigned to antigorite, whereas the 688 cm^{-1} band appears at a wavenumber higher than that of pure antigorite (683 cm^{-1}) or pure chlorite (682, 683 cm^{-1}). The shift indicates the presence of small amounts of chrysotile. The first band of the spectrum detected at 1088 cm^{-1}, and the remaining bands at 714 and 284 cm^{-1}, are assigned to calcite, whereas the spectral features at 552 and 358 cm^{-1} are due to chlorite (Prieto et al., 1991).

- The Raman spectrum of sample S4 shows the occurrence of antigorite and chrysotile. The bands at 1103, 692, 629, 464, 434, 390, and 347 cm^{-1} are attributed to chrysotile, whereas the bands typical of antigorite occur at 1044, 520, and 382 cm^{-1}. The band recorded at 232 cm^{-1} may be produced by both chrysotile and antigorite, while the peak at 321 cm^{-1} is related to chrysotile (Kloprogge et al., 1999).

Chemical Analysis. Representative chemical analyses of four samples from Pizzo Tremogge are summarized in table 4, together with the structural formula calculated on the basis of five oxygen atoms (O) and four hydroxide groups (OH). The (Si + Al) cations are sufficient to completely fill the tetrahedral site. The remaining Al is assigned, together with Ti^{4+}, Cr^{3+}, Fe^{2+}, Ni^{2+}, Mn^{2+}, Mg^{2+}, Ca^{2+}, Zn^{2+}, Na^{+}, and K^{+}, to the octahedral site.

The analyses are nearly stoichiometric, but we do observe a significant scatter in the composition, arising mainly from a variation in the aluminum and iron contents. This implies different substitutions of the cations for silicon and magnesium in the tetrahedral and octahedral sites, respectively. According to the data reported in the literature, these substitutions cause different crystal microstructures, playing a major role in stabilizing lizardite, chrysotile, or antigorite (e.g., Viti and Mellini, 1997).

The compositional patterns of Al_2O_3 and FeO observed in figure 8 show that in the four thin sections there is a general negative correlation of both oxides with silicon. In figures 8A and B, the analyses plot in two different areas. In fact, the S1 and S2 samples are enriched in Al_2O_3 and FeO and depleted in SiO_2 compared to the S3 and S4 samples. These compositional variations are related to the different serpentine species detected by Raman spectroscopy, although the occurrence of other minerals such as calcite, dolomite, and chlorite can also influence the microprobe measurement (Schwartz et al., 2013). In those four samples, the phases associated with serpentine minerals were chlorite, calcite, brucite, titanclinohumite (with a high TiO_2 content up to approximately 6 wt.%), and geikielite, the rare magnesian analogue of ilmenite. Minor amounts of titanium (TiO_2 = 0.03–

Figure 8. Plot of Al_2O_3 vs. SiO_2 (left), FeO vs. Al_2O_3 (center), and FeO vs. SiO_2 (right). Samples S1 and S2 are enriched in Al_2O_3 and FeO, as is common in lizardite. Samples S3 and S4 show the opposite behavior, consistent with their antigorite/chrysotile composition.

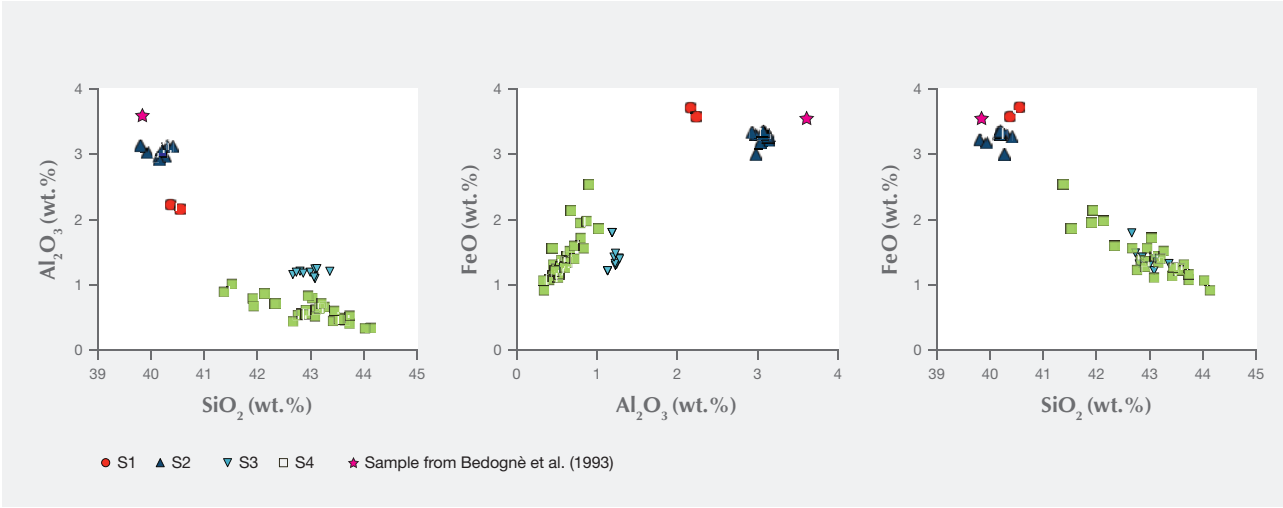

0.23 wt.%) and trace amounts of Ca, Cr, Ni, and Zn were also detected.

The chemical distinction between lizardite, chrysotile, and antigorite has been the subject of much speculation, and it remains an open question because the differences are very subtle. The grain size is also small, making it difficult to separate the various mineralogical phases for accurate analyses (Deer et al., 2009). According to the common interpretation, as well as the data from the literature (e.g., Viti and Mellini, 1997; Schwartz et al., 2013), lizardite is distinguished by its comparatively high Al content, whereas antigorite is always Al depleted, with Al_2O_3 never higher than 1 wt.% (Viti and Mellini, 1997). The SiO_2 content is generally lower in lizardite than in antigorite (Page, 1968). According to Viti and Mellini (1997), chrysotile has a wider compositional field, but its content of Al_2O_3 never exceeds 2 wt.%, regardless of SiO_2 content.

The chemical analyses of samples S1 and S2, as well as a previously reported sample of "noble" serpentine from Pizzo Tremogge (Bedogné et al., 1993), are enriched in Al and show a composition comparable to most of the lizardite analyzed by Viti and Mellini (1997). On the contrary, samples S3 and S4 showed depleted Al_2O_3 and enriched SiO_2, both typical features of antigorite. The broad variation of Al and Fe determined in these samples and the shifting of some analyses toward the compositional field of chrysotile (see the plot of FeO vs. Al_2O_3 in figure 8) could be due to the occurrence of this mineral or to a mixture of antigorite/chrysotile, as suggested by Raman spectroscopy.

CONCLUSIONS

This paper offers the first detailed mineralogical and gemological investigation of serpentine-group minerals from Pizzo Tremogge in Val Malenco, Italy. On the basis of Raman spectroscopy and chemical analyses, we have proved that the samples are generally composed of the main phases of the serpentine group: chrysotile, lizardite, and antigorite. The occurrence of minor phases, such as carbonates, quartz, brucite, and chlorite, leads to a pleasing color variation in the cut gems, which is preferred in the Italian market over uniform colors.

It is well documented that serpentine minerals play an important role in the interpretation of many geological and petrological processes. Due to their different stability fields, which are strongly *P/T* dependent, their coexistence in the marbles of Pizzo Tremogge may provide a fundamental basis for understanding the complex metamorphic processes and geological setting of the Val Malenco area. In particular, the presence of antigorite suggests that the marbles at Pizzo Tremogge have experienced a high grade of metamorphism at temperature above approximately 320°C, at which antigorite crystals overprinted earlier-formed serpentine minerals such as lizardite and/or chrysotile.

ABOUT THE AUTHORS

Dr. Adamo (ilaria.adamo@igi.it) is a staff member of the Italian Gemological Institute (IGI) in Milan and a collaborator in the earth science department of the University of Milan. Dr. Bocchio is a professor of mineralogy, and Dr. Marinoni is a researcher, at the University of Milan. Dr. Diella is a senior researcher at the National Research Council, IDPA, Milan Organizational Support Unit. Dr. Rinaudo is professor of mineralogy in the department of science and technology innovation at the University of Eastern Piedmont in Alessandria, Italy.

ACKNOWLEDGMENTS

The authors would like to thank Mr. Pietro Nana (Sondrio, Italy) for providing samples and useful information. Microprobe analyses were performed at the earth science department of the University of Milan with the technical assistance of Mr. Andrea Risplendente.

REFERENCES

Adamo I., Bocchio R. (2013) Nephrite jade from Val Malenco, Italy: Review and update. *G&G*, Vol. 49, No. 2, pp. 98–106, http://dx.doi.org/10.5741/GEMS.49.2.98

Adamo I., Bocchio R., Diella V., Pavese A., Vignola P., Prosperi L., Palanza V. (2009) Demantoid from Val Malenco, Italy: Review and update. *G&G*, Vol. 45, No. 4, pp. 280–287, http://dx.doi.org/10.5741/GEMS.45.4.280

Adamo I., Diella V., Bocchio R., Marinoni N., Mainardi M., Fontana E., Rinaudo C. (2014) "Noble serpentine": a case study from Val Malenco, Central Alps, Italy. *Plinius*, Vol. 40, p. 329.

Bedogné F., Montrasio A., Sciesa E. (1993) *I Minerali della Provincia di Sondrio: Valmalenco*. Bettini, Sondrio, Italy.

Choudhary G. (2009) Gem News International: Serpentine cat's eye. *G&G*, Vol. 45, No. 2, pp. 151–152.

Deer W.A., Howie R.A., Zussman J. (2009) *Rock-Forming Minerals, Volume 3B: Layered Silicates Excluding Micas and Clay Minerals.* The Geological Society, London, 314 pp.
Diella V., Adamo I., Bocchio R. (2014) Gem-quality rhodonite from Val Malenco (Central Alps, Italy). *Periodico di Mineralogia*, Vol. 83, No. 2, pp. 207–221, http://dx.doi.org/10.2451/2014PM0012
Evans B.W., Hattori K., Barronet A. (2013) Serpentinite: what, why, where? *Elements*, Vol. 9, No. 2, pp. 99–106, http://dx.doi.org/10.2113/gselements.9.2.99
Fubini B., Fenoglio I. (2007) Toxic potential of mineral dust. *Elements*, Vol. 3, No. 3, pp. 407–414, http://dx.doi.org/10.2113/gselements.3.6.407
Gramaccioli C.M. (1962) *I minerali valtellinesi nella raccolta di Pietro Sigismund* [*The Minerals in the Valtellina Collection of Pietro Sigismund*]. Fusi, Pavia, Italy, 179 pp. (in Italian).
Groppo C., Rinaudo C., Cairo S., Gastaldi D., Compagnoni R. (2006) Micro-Raman spectroscopy for a quick and reliable identification of serpentine minerals from ultramafics. *European Journal of Mineralogy*, Vol. 18, No. 3, pp. 319–329, http://dx.doi.org/10.1127/0935-1221/2006/0018-0319
Guillot S., Hattori K. (2013) Serpentinites: Essential roles in geodynamics, arc volcanism, sustainable development, and the origin of life. *Elements*, Vol. 9, No. 2, pp. 95–98, http://dx.doi.org/10.2113/gselements.9.2.95
Kim W.-S., Ahn H.-J., Kim D.-H., Yoon S.-H. (2006) Mineralogy and genesis of gem-quality serpentine jade from Korea. Geological Society of America, *Abstract with Programs*, Vol. 38, p. 93, https://gsa.confex.com/gsa/2006CD/webprogram/Paper102570.html
Kloprogge J.T., Frost R.L., Rintoul L. (1999) Single crystal Raman *microscopic study of asbestos mineral chrysotile. Physical Chemistry Chemical Physics*, Vol. 1, No. 10, pp. 2559–2564, http://dx.doi.org/10.1039/A809238I
Lin Xinying, Lin Xianzhou, Shuyi Y. (2012) Research on Serpentine Jade in Jilin Province. 2012 International Conference on Solid State and Materials. *Lecture Notes in Information Technology*, Vol. 22, pp. 96–100.
Müntener O., Hermann J., Trommsdorff V. (2000) Cooling history and exhumation of lower-crustal granulite and upper mantle (Malenco, Eastern Alps). *Journal of Petrology*, Vol. 41, No. 2, pp. 175–200, http://dx.doi.org/10.1093/petrology/41.2.175
O'Donoghue M. (2006) *Gems*, 6th ed. Butterworth-Heinemann, Oxford, UK.
Page N.J. (1968) Chemical differences among the serpentine "polymorphs." *American Mineralogist*, Vol. 53, No. 1–2, pp. 201–205.
Petriglieri J.R., Salvioli-Mariani E., Mantovani L., Tribaudino M., Lottici P.P., Laporte-Magoni C., Bersani D. (2015) Micro-Raman mapping of the polymorphs of serpentine. *Journal of Raman Spectroscopy*, Vol. 46, No. 10, pp. 953–958, http://dx.doi.org/10.1002/jrs.4695
Prieto A.C., Dubessy J., Cathelineau M. (1991) Structure-composition relationships in trioctahedral chlorites: a vibrational spectroscopy study. *Clays and Clay Minerals*, Vol. 39, No. 5, pp. 531–539.
Rinaudo C., Gastaldi D., Belluso E. (2003) Characterization of chrysotile, antigorite and lizardite by FT-Raman spectroscopy. *The Canadian Mineralogist*, Vol. 41, No. 4, pp. 883–890, http://dx.doi.org/10.2113/gscanmin.41.4.883
Schwartz S., Guillot S., Reynard B., Lafay R., Debret B., Nicollet C., Lanari P., Auzende A.L. (2013) Pressure-temperature estimates of the lizardite/antigorite transition in high pressure serpentinites. *Lithos*, Vol. 178, pp. 197–210, http://dx.doi.org/10.1016/j.lithos.2012.11.023
Viti C., Mellini M. (1997) Contrasting chemical compositions in *associated lizardite and chrysotile in veins from Elba, Italy. European Journal of Mineralogy*, Vol. 9, No. 3, pp. 585–596, http://dx.doi.org/10.1127/ejm/9/3/0585
White S.N. (2009) Laser Raman spectroscopy as a technique for identification of seafloor hydrothermal and cold seep minerals. *Chemical Geology*, Vol. 259, No. 3–4, pp. 240–252, http://dx.doi.org/10.1016/j.chemgeo.2008.11.008